EXCITON SPECTRA AND ENERGY BAND STRUCTURE OF $CuAlSe_2$ CRYSTALS

N. N. Syrbu[1], A. V. Dorogan[1], A. Masnik[1], and V. V. Ursaki[2]

[1]*Technical University of Moldova, Stefan cel Mare str. 168, Chisinau, MD-2004 Republic of Moldova*

[3]*Institute of Applied Physics of the Academy of Sciences of Moldova, Academiei str. 5, Chisinau, MD-2028 Republic of Moldova*

(Received 8 April 2011)

Abstract

The main exciton parameters and the refined values of the energy intervals $V_1(\Gamma_7)$ - $C_1(\Gamma_6)$, $V_2(\Gamma_6)$ - $C_1(\Gamma_6)$ and $V_3(\Gamma_7)$ - $C_1(\Gamma_6)$ in $CuAlSe_2$ crystals are discussed. The crystal field and spin-orbit splitting of the balance band are determined. The effective masses of electrons (m^*_{C1}), and holes (m^*_{V1}, m^*_{V2}, m^*_{V3}) are estimated. The contours of reflectivity spectra at high photon energies (E > Eg) are calculated on the basis of Kramers-Kronig relations. The spectral dependences of the real and imaginary parts of the dielectric function, of the refractive indexes n_o, n_e, and the absorption coefficient were determined. The experimental data are discussed on the basis of theoretical band structure calculations.

1. Introduction

$CuAlSe_2$ compound belongs to the I-III-VI_2 group semiconductors and crystallizes into a chalcopyrite structure with the space group $I^4_{2d} - D^{12}_{2d}$. The materials from this group present interest for applications in optoelectronic devices, particularly, for the development of solar cells [1-3]. The photoluminescence properties of $CuAlSe_2$ crystals doped with Er^{3+} ions [3] and the photoelectrical properties of surface barrier structures based on $CuAlSe_2$ crystals have been previously investigated [4–6]. These compounds possess a strong anisotropy of optical properties both in the visible and infrared spectral range.

Some optical and transport measurements were carried out on $CuGaSe_2$ thin films and single crystals [7-16]. The values of the fundamental gap and its temperature dependence, the crystal field and spin-orbit valence band splitting, as well as phonon and exciton parameters and the defect level schema were reported. The energy band structure of the I-III-VI compounds has been calculated as the nearest zincblende analogue [17, 18].

In this paper, we investigate the exciton spectra and the electronic transitions in a wide energy range in $CuAlSe_2$ crystals. The electronic transitions are discussed on the basis of previously performed theoretical band structure calculations.

2. Experimental methods

Platelike $CuAlSe_2$ crystals with 2.5 x 1.0 cm^2 mirror surfaces and 300–400 μm thickness were grown by vapor phase transport. The surfaces of some platelets were parallel to the C axis. The optical transmission and reflectivity spectra were measured with a MDR-2 spectrometer. The samples were mounted on the cold station of an LTS-22 C 330 optical cryogenic system for low-temperature measurements.

3. Analysis of the band structure of $CuAlSe_2$ crystals at the center of the Brillouin zone

According to theoretical calculations of the energy band structure, the band-gap minimum in $CuAlSe_2$ crystals is formed by direct electronic transitions in the center of the Brillouin zone [19, 20]. The lower conduction band is of Γ_6 symmetry, while the upper V_1, V_2, V_3 valence bands are of Γ_7, Γ_6 and Γ_7 symmetry, respectively. The interaction of electrons from the conduction band Γ_6 (C_1) with holes from the valence band Γ_7 (V_1) is determined by the product of irreducible representations $\Gamma_1 \times \Gamma_6 \times \Gamma_7 = \Gamma_3 + \Gamma_4 + \Gamma_5$. A Γ_4 exciton allowed in the E||c polarization, a Γ_5 exciton allowed in the E⊥c polarization, and a Γ_3 exciton forbidden in both polarizations are formed in the long-wavelength region as a result of this interaction. The interaction of a hole from the Γ_6 band with an electron from the Γ_6 band leads to the formation of three exciton series with Γ_1, Γ_2 and Γ_5 symmetries. The Γ_5 excitons are allowed, while Γ_1 and Γ_2 excitons are forbidden in E⊥c polarization according to the selection rules [12, 21].

The n = 1 (ω_t = 2.8212 eV, ω_L = 2.8237 eV) and n = 2 (2.8390 eV) lines as well as a weak line at 2.8442 eV of the Γ_4 exciton hydrogen-like series are observed in the reflectivity spectra of $CuAlSe_2$ crystals measured at 10 K in the E‖c, k⊥c polarization. These lines are discussed in [22]. The reflectivity spectra in the region of the n = 1 line are of a usual excitonic shape with a maximum and a minimum. These peculiarities are due to presence of the transversal and longitudinal excitons. A longitudinal-transversal exciton splitting of 2.5 meV is estimated for the Γ_4 excitons from these data. A Rydberg constant of 24 meV is determined for the Γ_4 exciton series from the position of n = 1 and n = 2 lines. The energy of the continuum (E_g, $n = \infty$) is 2.845 eV. These energy values of the ground (n = 1) exciton states are in a satisfactory accordance with previously reported values measured at 77 K for A-, B- and C-excitons, respectively [22, 23].

The background dielectric constant ε_d was estimated from the measurements of reflectivity in the IR (400 cm^{-1}) and near-IR (12000 cm^{-1}) regions [22, 24]. The reported value of ε_b in $CuAlSe_2$ crystals equals 6.67 in the (E‖c) polarization and 8.28 in the (E⊥c) polarization far from the exciton resonances (ν = 4000-3000 cm^{-1}) [24]. The coefficient of reflection equals 0.24-0.25, and the value of ε_b is 7.4-8.2 in the region of exciton resonances. The value of the background dielectric constant near the exciton resonance was used in calculations. With ε_b = 7.6 and Rydberg constant R =0.024 eV, the Γ_4-exciton reduced mass equals to $\mu = \varepsilon_b^2 R/R_H = 0.1m_0$, where R_{H_2} is the Rydberg energy of the hydrogen atom (13.6 eV). The Bohr radius (a_B) of the S-state of the Γ_4-exciton equals $0.3x10^{-6}$ cm. A maximum at 2.851 eV (transversal exciton) and a minimum at 2.853 eV (longitudinal exciton) are observed in the E⊥c polarization for the Γ_5 exciton series. The longitudinal-transversal splitting of the Γ_5 exciton equals 2.0 meV. The n=2 excited exciton state is observed at 2.868 eV. The binding energy of the Γ_5 exciton equals 22 meV, and the energy of the continuum equals 2.873 eV. The C-exciton is observed at 3.023 eV (n=1) and 3.039eV ($n=2$) in the same polarization. The Rydberg constant equals 18 meV, and the energy of the continuum equals 3.044 eV for this exciton.

The calculations of the reflectivity spectra in [22] were carried out within the framework of classical optics taking into account the spatial dispersion and the presence of a dead-layer [25-29]. The translation mass M of the Γ_4 and Γ_5 excitons equal to $1.3m_0$ were determined from these calculations in $CuAlSe_2$ crystals

The values of the reduced mass of excitons are determined from the relation

$$\mu = \frac{\varepsilon_b^{\parallel} \varepsilon_b^{\perp} R_j}{R_{H_2}}, \tag{1}$$

where j corresponds to Γ_4 and Γ_5 excitons, R_j is the binding energy of the j-exciton, R_{H_2} is the Ridberg constant of the hydrogen atom, $\varepsilon_b^{\parallel}$ and $\varepsilon_b^{\perp}$ are the background dielectric constants. The effective masses in the conduction and three valence bands were determined on the basis of these data, and taking into account that $M = m_v^* + m_c^*$ and $1/\mu = 1/m_v^* + 1/m_c^*$, where m_c^*, $m_{v1\text{-}3}^*$ are the effective masses in the conduction band and in the $\Gamma_7(V_1)$, $\Gamma_6(V_2)$, $\Gamma_7(V_3)$ valence bands.

With the values of $M = 1.3m_0$ and $\mu = 0.1m_0$, the electron effective mass m_c^* equals $0.11m_0$, and the effective mass of holes m_{v1}^* equals $1.2m_0$. These values of the effective masses do not differ significantly from those obtained previously for $CuGaSe_2$ crystals. The parameters of the Γ_5 excitons do not essentially differ from the parameters of Γ_4 excitons.

With the translation mass $M = (0.5 – 0.8)m_0$ and the B-exciton binding energy $R = 22$ meV, the electron effective mass m_c^* equals $0.11m_0$, and the effective mass of light holes m_{v2}^* equals $(0.4 – 0.7)m_0$. For the C-exciton series, the reduced effective mass equals $\mu = 0.076m_0$, and the m_{v3}^* hole mass equals $0.25m_0$. The parameters of energy bands are presented in Fig. 1.

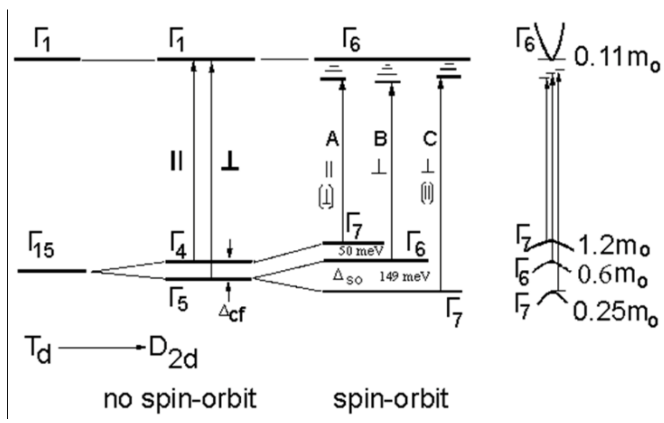

Fig. 1. Energy band structure at the Γ point illustrating the transition from the zincblende (T_d) to the chalcopyrite (D_{2d}) structure.

The parameters of the exciton series and the energy of the continuum (E_g) [22] makes it possible to reliably determine the splitting of the upper valence bands at the center of the Brillouin zone due to the crystal field (Δ_{cf}) and spin-orbit interaction (Δ_{so}).

As mentioned above, the energy band structure of the I-III-VI compounds was calculated as the nearest zincblende analogue [19, 20]. A stronger decrease in the bandgap and the spin-orbit splitting is found as compared to the zincblende analogs. In most of crystals from this group, including $CuAlSe_2$, the bandgap is decreased by 1 eV as compared to the ZnSe analog, and the spin-orbit splitting decreases from 0.45 eV to 0.23 eV. These effects are explained by the hybridization of the p- and d-states, which determine the upper valence bands at the center of the Brillouin zone [19, 20].

The interval between the levels $\Gamma_7(V_1) – \Gamma_6(V_2)$ in I-III-VI_2 structures is assigned as E_1, and the interval between the levels $\Gamma_6(V_2) - \Gamma_7(V_3)$ is assigned as E_2 provided that $\Delta_{cf} < E_g$. These values are deduced from the Hamiltonian matrix and are determined by the following relation:

$$E_{1(2)} = \frac{1}{2}\left(\Delta_{so} + \Delta_{cf}\right) \pm \left[\frac{1}{4}\left(\Delta_{so} + \Delta_{cf}\right)^2 - \frac{2}{3}\Delta_{so}\Delta_{cf}\right]^{1/2}. \tag{2}$$

By using this relation and taking into account the energy position of the n = 1 lines of the A, B, and C excitons, we can calculate the value of the crystal field and spin-orbit splitting. Table 1 summarizes the calculated values of the Δ_{cf} and Δ_{SO} from the position of ground (*n* = 1) states of the A, B и C excitons in $CuAlSe_2$.

Table 1. Exciton parameters of $CuAlSe_2$ crystals

		A(eV)	B(eV)	C(eV)	Δ_{cf} (meV)	Δ_{so} (meV)
Exciton state	n=1	2.821	2.851	3.023		
	n=2	2.839	2.868	3.039		
	R	0.024	0.022	0.018		
E_g (n=∞)		2.845	2.873	3.041	-49.6	149

Previously [19, 30], the crystal field splitting has been estimated from the following relation:

$$\Delta_{kp} = -3/2b\left(2 - c/a\right) \tag{3}$$

where *a* and *c* are the crystal lattice constants, b is the deformation potential, which equals 1.0 for the I-III-VI_2 chalcopyrite compounds. The following relation is used for the estimation of the influence of the p-d hybridization on the spin-orbit splitting:

$$\Delta_{SO} = \beta\Delta_p + \left(1-\beta\right)\Delta_d \tag{4}$$

where the spin-orbit splitting of the *p*-states equals Δ_p = 0.43 eV for the Cu atoms, and Δ_d = -0.13 eV is the negative spin-orbit splitting of the d-levels, β is the content of the *p*-states in the upper bands in percents [19, 30]. Using these relations, the income of the p- and d-states in the upper valence bands of $CuAlSe_2$ crystals was estimated to be around 23-30% and 70-77%, respectively.

4. Calculation of optical functions from the reflection spectra using the Kramers-Kronig relations

The measurement of the coefficient of reflection, i.e. the amplitude of the Fresnel coefficient of reflection, in the wide energy interval in the case of a normal incidence makes it possible to determine the phase of the reflected radiation beam. According to [31, 32] the coefficient of reflection can be presented as

$$r = \frac{n - ik - 1}{n - ik + 1} = \sqrt{R}e^{-i\varphi}, \tag{5}$$

where *R* is the coefficient of reflection at a normal incidence angle, *n* is the refraction index, *k* is the extinction index, and φ is the phase angle. The Kramers-Kroning relations describe the relation between the phase and the amplitude of the complex Fresnel coefficient of reflection at a normal incidence angle [31, 32]:

$$\varphi(\omega_0) = \frac{\omega_0}{\pi} \int_0^{\infty} \frac{\ln R(\omega)}{\omega_0^2 - \omega^2} d\omega . \tag{6}$$

To calculate the exact value of φ, it is necessary to have the spectrum of the index of reflection in an infinite frequency interval, while the real experimental spectrum is measured in a limited frequency interval $a \le \omega \le b$.

In the present work, the reflectivity spectra of $CuAlSe_2$ crystals are measured in the energy interval of 2.5 to 6 eV with a polarized light. A structure of maxima (a_1-a_{10}, e_1-e_9) associated with interband transitions at different points of the Brillouin zone is observed in the reflectivity spectrum measured at energies $E > E_g$ at 77K in $E \| c$ and $E \perp c$ polarization (Fig. 2). As previously proposed [17, 18], the φ values in the high energy region ($b \le \omega \le \infty$), where the spectra were not measured, were calculated by means of an extrapolation of the spectral dependence of the coefficient of reflection by using the function $R(\omega) = c\omega^{-p}$, where C, p are some constants [31, 32]. The $R(\omega) = R(a)$ approximation was used in the region of $0 \le \omega \le a$ without taking into account the contribution of lattice vibrations to the coefficient of reflection in this spectral interval.

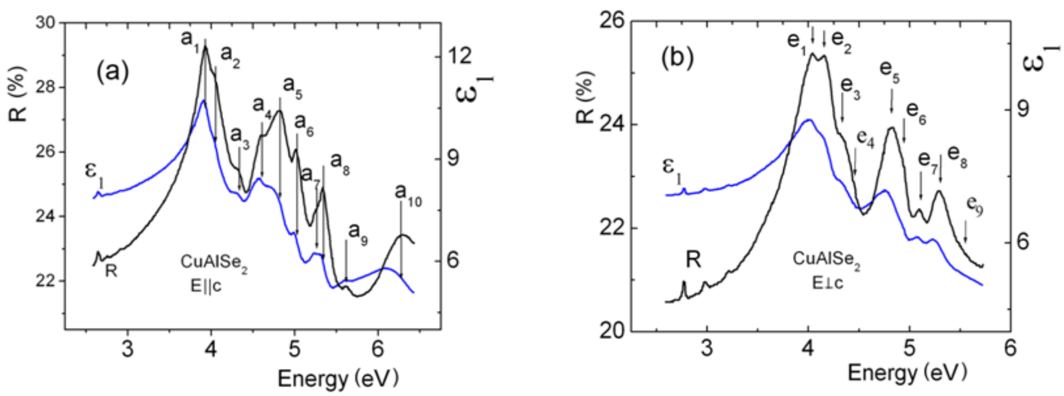

a) b)

Fig. 2. Spectra of the coefficient of reflection R and the real part of the dielectric permeability $\varepsilon_1(\omega)$ obtained from the calculations of the reflectivity spectra using Kramers-Kronig relations for $CuAlSe_2$ crystals for E||c polarization (a) and E⊥c polarization (b).

The optical functions have been determined by using the calculated φ values and the experimental values of R:

$$n = \frac{1-R}{1-2\sqrt{R}\cos\varphi + R} \qquad k = \frac{2\sqrt{R}\sin\varphi}{1-2\sqrt{R}\cos\varphi + R} \qquad \varepsilon_1 = n^2 - k^2 \text{ and } \varepsilon_2 = 2nk . \tag{7}$$

Figure 2 presents the spectra of the coefficient of reflection R and the real part of the dielectric permeability $\varepsilon_1(\omega)$ obtained from the calculations of the reflectivity spectra using the Kramers-Kronig relations for $CuAlSe_2$ crystals for E||c and E⊥c polarization. As expected, the maxima of the coefficient of reflection correspond to the short-wavelength decrease of the ε_1 function.

Figure 3 shows the spectral dependences of the imaginary part ε_2 of the dielectric permeability for both polarizations. As one can see from the figure, the curves of the spectral dependences of ε_2 for E||c and E⊥c polarizations intersect at energies of 2.8, 4.3, and 5.4 eV.

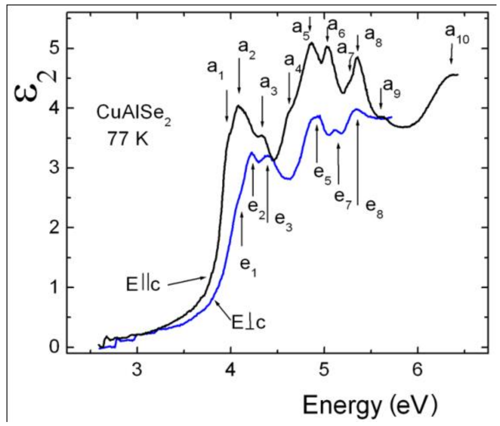

Fig. 3. The imaginary part of the dielectric permeability $\varepsilon_2(\omega)$ for E║c and E⊥c polarizations for $CuAlSe_2$ crystals.

Figure 4 presents the spectral dependence of the refractive index *n* and the extinction coefficient *k* calculated using relations (5)-(7). The optical functions of $CuGaS_2$, $CuInS_2$, and $CuGaSe_2$ crystals were calculated by using this method [17, 18]. The results of these calculations are in good agreement with the earlier published results on ellipsometry of these crystals [33-36].

The anisotropy of spectral dependences of ε_1, ε_2, *n*, and *k* is observed in $CuAlSe_2$ crystals in E||c and E⊥c polarizations (Fig. 4). Similar values of *n* (2.66-2.82) were obtained in an interval of 1.9-2.5 eV in $CuGaS_2$ single crystals [33, 18]. The values of the refractive index in E||c and E⊥c polarizations at an energy of 2.1 eV are 2.720 and 2.724 eV, respectively [18]. The reported values of *n* and *k* for thin films of $CuInS_2$ are different depending on the method of crystal growth, they being as follows: *n*= 2.65-3.05 (0.5-3.0 eV), *k*= 0-1.18 (1.35-3 eV) [34]; *n* = 2.72-2.95 (0.8-1.4 eV), *k* = 0.22-0.42 (1.7-1.9 eV) [35]; and *n*= 2.3-1.8 (1.5-4.0 eV), *k* = 0.45-0.8 (1.5-4.0 eV) [36].

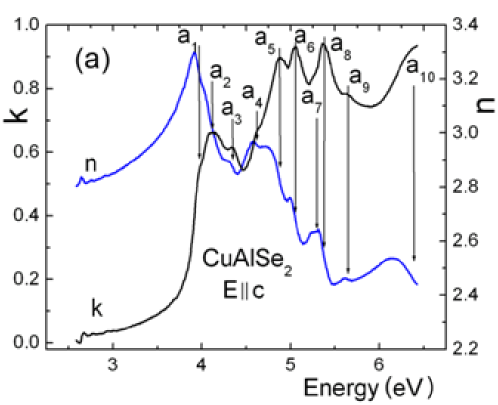

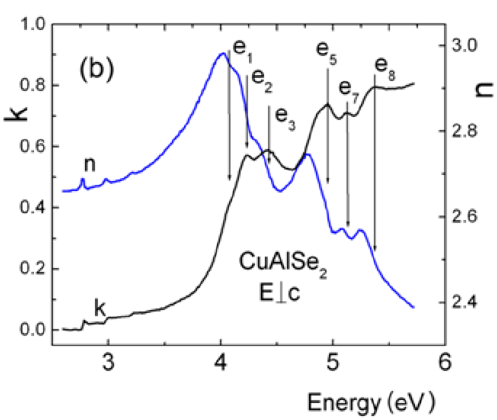

Fig. 4. Spectral dependences of the refractive index (n) and extinction coefficient (k) of $CuAlSe_2$ single crystals at E║c and E⊥c polarizations.

In order to analyze the anisotropy of the refractive index, Fig. 5 presents the spectral dependence of the refractive index of $CuAlSe_2$ crystals for E||c (n_o) and E⊥c polarizations (n_e). The intersection of the dispersion curves of the ordinary (n_o) and extraordinary (n_e) refractive indexes at a certain wavelength λ_0 is a peculiarity of uniaxial crystals. The uniaxial crystal exhibits a behavior of optical isotropic medium at the wavelength $\lambda = \lambda_0$, and this wavelength is called "isotropic wavelength" or isotropic point (IP). Actually, a lot of crystals with isotropic wavelength were investigated [21-32]. However, the isotropic wavelength was investigated mainly in the region of the fundamental absorption edge [27-29, 32].

The isotropic wavelength in the region of transparency for different crystals is as follows: 536 nm in $CuAlSe_2$, 642 nm in $CuGaS_2$, 811 nm in $AgGaSe_2$, 810 nm in $CuGaSe_2$ [23, 24]. The transmission spectra of these crystals placed between two cross-oriented polarizers with the optical axis parallel to polarization of one of the polarizers represents a narrow transmission band localized at the wavelength of IT (band pass mode filter) [25-32]. By the contrary, in the case of a uniaxial crystals placed between two parallel-oriented polarizers, a narrow absorption band is observed in the transmission spectrum (band elimination filter). The peculiarity of crystals is used for the filtration of optical radiation [25-32]. The platelets of $AgGaS_2$ with optical isotropy wavelength ("null wavelength" plates) were used for manufacturing Lyot filters and Solc filters [25, 26].

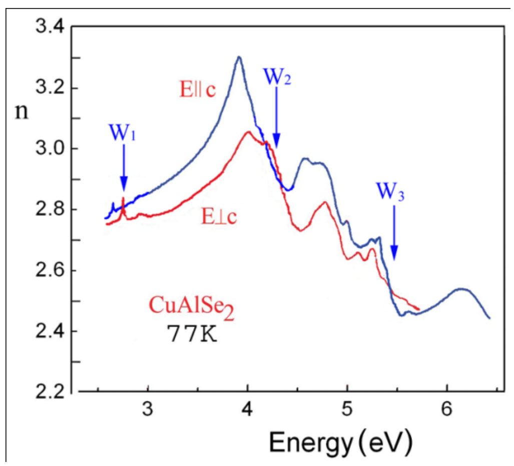

Fig. 5. Spectral dependences of the refractive index (n) of $CuAlSe_2$ single crystals at E$\|$c and E$\perp$c polarizations.

Materials with a chalcopyrite structure possess a higher birefringence as compared to crystals with a wurtzite structure. The difference between the optical isotropy wavelength λ_o and the fundamental absorption edge in semiconductors with a chalcopyrite structure is higher as compared to wurtzite semiconductors.

We demonstrate in this paper that this peculiarity of crystals can be also observed in the region of fundamental absorption. This is clearly observed by comparing the spectral dependence of ε_2 (Fig. 3), the refractive index *n*, and the extinction coefficient *k* (Fig. 4) obtained from the calculation of reflectivity spectra in the exciton region and deep in the absorption band. These wavelengths are marked with W1, W2, and W3 in Fig. 5. The presence of isotropic wavelengths in the region of fundamental absorption is very important actually in connection with the development of device structures with nanolayers. The development of structures with nanolayers based on semiconductors with isotropic wavelength makes it possible to control the optical waves in the high energy spectral region as well as in the region of the absorption edge [25-32].

The spectral dependence of the absorption coefficient determined as $\alpha(\lambda) = \frac{4\pi}{\lambda} k(\lambda)$ is of a major importance for the development of solar cells and optoelectronic photodetectors. The higher is the value of the absorption coefficient in the fundamental absorption region, the higher is the amount of energy converted into electricity.

Figure 6 presents the absorption spectra in the region of $E>E_g$ obtained from the calculation of transmission and reflection spectra of $CuAlSe_2$ crystals. One can see that the value of the absorption coefficient is rather high in both the polarizations of the light wave. The anisotropy of the absorption coefficient α and the presence of isotropic wavelengths (W1, W2 and W3) in these crystals can be used for the development of current sign inverters [37] with nanolayer active regions working in the region of isotropic wavelengths.

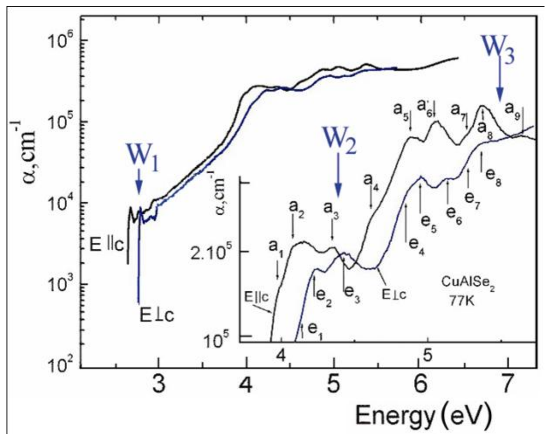

Fig. 6. Spectral dependence of the absorption coefficient of $CuAlSe_2$ crystals at E║c and E⊥c polarization at 77 K.

5. Electronic transitions and the energy band structure of $CuAlSe_2$ crystals

The electronic transitions revealed in experimental reflectivity spectra and in ellipsometry of I-III-VI_2 crystals are interpreted on the basis of theoretical calculations [19] conducted for the T, Γ, and N points of the Brillouin zone. Apart from that, theoretical calculations of the band structure were performed for other points of the Brillouin zone, such as Z, X, and P [20], and compared with experimental data [19].

The features observed in the experimental reflectivity spectra of $CuInS_2$, $CuGaS_2$ [18], and $CuGaSe_2$ [17], as well as in the calculated spectral dependences of the imaginary $\varepsilon_2(\omega)$ and real $\varepsilon_1(\omega)$ parts of the dielectric permeability, are due to direct electronic transitions at different points of the Brillouin zone. The experimentally determined values of the energy intervals are compared to the calculated band structure at the Γ, P, X, Z, and N points of the Brillouin zone [20].

The energy band structure in the neighborhood of Z, X, and P points was calculated without taking into account the spin-orbital and the crystal field interaction. The valence bands are degenerated at these points. Actually, the valence bands are split which results in a large number of polarized electronic transitions revealed in the reflectivity spectra. For instance, two upper valence bands V_1, V_2 are evidenced at the Z point. Each of these bands is twofold degenerated. As a result, there are four electronic transitions to the C_1 conduction band at the Z point. A similar situation occurs at other points of the Brillouin zone. The maxima A_i, E_i emerge in the reflection spectra as a result of the degeneration removal of V_1 bands at different points of the Brillouin zone.

Intense a_1-a_{10} and e_1-e_9 maxima are observed in the reflectivity spectra of $CuAlSe_2$ crystals measured in E||c and E⊥c polarizations in the region of $E>E_g$ (Fig. 2). Some features were observed in a region of 2.5, 3.5, and 4.5 eV in the ellipsometry measurements performed at room temperature in $CuAlSe_2$ crystals [38]. These features are better resolved with decreasing the temperature. By analogy with A_1, E_1 transitions observed in $CuInS_2$, $CuGaS_2$ and $CuGaSe_2$ crystals previously observed in E||c and E⊥c polarizations, respectively [17, 18], we attribute the maxima observed in the spectral dependence of the R/ε at 3.921/3.905 eV (a_2) in E||c polarization and 4.045/4.045 eV (e_2) in E⊥c polarization to $\Gamma_7(V_1)$-$\Gamma_6(C_1)$ electronic transitions (Table 2).

Table 2. The interpretation of interband transitions in $CuAlSe_2$ crystals and the values of the respective energy intervals deduced from measurements of the reflectivity spectra (R) or dielectric permeability spectra (ε). The values of the damping parameter (γ) are also presented.

a_1	R	3.921	$\Gamma_7(V_1)$- $\Gamma_7(C_2)$	a_6	R	5.017	$X(V_2)$-$X(C_1)$
	ε	3.905			ε	5.008	
	γ	0.07(1)			γ	0.10(1)	
e_1	R	4.045		e_6	R	4.932	
	ε	4.045			ε	4.932	
	γ	0.06(1)			γ	0.05(2)	
a_2	R	4.045	$\Gamma_6(V_2)$- $\Gamma_7(C_2)$	a_7	R	5.261	$N(V_1)$- $N(C_1)$
	ε	4.045			ε	5.261	
	γ	0.07(1)			γ	0.10(2)	
e_2	R	4.157		e_7	R	5.104	
	ε	4.157			ε	5.104	
	γ	0.04(1)			γ	0.09(1)	
a_3	R	4.299	$Z(V_1)$-$Z(C_1)$ or $P(V_1)$-$P(C_1)$	a_8	R	5.331	$N(V_2)$- $N(C_1)$
	ε	4.299			ε	5.331	
	γ	0.04(2)			γ	0.14(3)	
e_3	R	4.314		e_8	R	5.290	
	ε	4.314			ε	5.290	
	γ	0.04(1)			γ	0.1(1)	
a_4	R	4.596	$Z(V_2)$-$Z(C_1)$ or $P(V_2)$-$P(C_1)$	a_9	R	5.602	$N(V_3)$- $N(C_1)$
	ε	4.585			ε	5.602	
	γ	0.07(1)			γ	0.07(1)	
e_4	R	4.464		e_9	R	5.491	
	ε	4.464			ε	5.491	
	γ	0.05(2)			γ	0.06(2)	
a_5	R	4.797	$X(V_1)$-$X(C_2)$	a_{10}	R	6.276	
	ε	4.788			ε	6.234	
	γ	0.07(2)			γ		
e_5	R	4.821		e_{10}	R		
	ε	4.821			ε		
	γ	0.08(1)			γ		

The maxima a_2 (4.045/4.045 eV) and e_2 (4.157/4.157 eV) are observed in the short-wavelength region of the a_1, e_1 maxima in E||c and E⊥c polarizations, respectively. The difference of energies of a_2, e_2 and a_1, e_1 maxima is nearly equal to the splitting of the valence bands in the center of the Brillouin zone (123-150 meV) due to the crystal field and spin-orbital interaction. Therefore, the a_2, e_2 maxima are also assigned to the electronic transitions in the center of the Brillouin zone from the $\Gamma_7(V_3)$ valence band to the $\Gamma_7(C_2)$ conduction band.

Two peaks a_3 (4.299/4.299 eV) and e_3 (4.314/4.314 eV) are observed in spectra of $CuAlSe_2$ in E||c and E⊥c polarizations, respectively. An analogous maximum A_3 was observed at 3.55 eV in unpolarized spectra of $CuGaSe_2$ crystals [17]. This maximum was assigned to $N_1(V_3)$-$N_1(C_1)$ transitions. Similar transitions were observed at 3.50 eV ($E_1(\Delta X)$ XΓ) in ellipsometry spectra of $CuGaSe_2$ crystals measured at 300 K in E||c polarization [38, 39]. These ellipsometry data were treated in terms of $\Gamma_5(V)$- $\Gamma_1(C)$ transitions. The energy intervals between the upper valence band and the lower conductance band in $CuGaSe_2$ crystals in the neighborhood of P and Z points equal to 2.04 E_0, where E_0 is the minimum energy interval at the Γ point, while this interval is of 2.43E_0 at the N point according to the estimations of [17].

The energy intervals in the neighborhood of P and Z points are significantly narrower than the respective intervals at the N point. On the basis of these data, one can assign the maxima A_3, E_3 and A_4, E_4 in the reflectivity spectra of $CuGaSe_2$ crystals to the transitions at the P and Z points. On the basis of these data, one can suggest that the peaks a_3 (4.299/4.299 eV) and e_3 (4.314/4.314 eV) observed in spectra of $CuAlSe_2$ crystals in E||c and E⊥c polarizations are due to $Z(V_1)$-Z (C_1) or $P(V_1)$-$P(C_1)$ transitions, while the peaks a_4 (4.596/4.585 eV) and e_4 (4.464/4.464 eV) are due to $Z(V_2)$-$Z(C_1)$ or $P(V_2)$-$P(C_1)$ transitions (Table 2).

The maxima A_5 (4.08/4.11 eV) and E_5 (4.08/4.10 eV) were observed in a region of 4 eV in $CuGaSe_2$ crystals in E||c and E⊥c polarizations, respectively. A maximum A_5 was also observed at 4.10 eV in the reflectivity spectra of $CuGaSe_2$ crystals which was attributed to $\Gamma_7(V_1)$- $\Gamma_2(C_3)$ transitions. These maxima are analogous to the (E_1(B)) peaks observed at 4.05 eV (E||c) and 4.03 eV (E⊥c) in the ellipsometry spectra measured at 300 K [39] which were attributed to $N_1(V_2)$-$N_1(C_1)$ transitions. According to recent theoretical calculations [20], the interband intervals at the X point are higher as compared to those at the P and Z points, but they are smaller as compared to those at the N and T points. Therefore, the maxima A_5 (4.11 eV) and E_5 (4.10 eV) in spectra of $CuGaSe_2$ crystals [17] were assigned to transitions from the V_1 band to the C_1 band at the X point. Similarly, the peaks a_5 (4.797/4.788 eV) and e_5 (4.821/4.821 eV) observed in spectra of $CuAlSe_2$ crystals can be attributed to $X(V_1)$-$X(C_2)$ transitions.

The maxima a_6 (5.017/5.008 eV) and e_6 (4.932/4.932 eV) observed in $CuAlSe_2$ crystals in E‖c and E⊥c polarizations, respectively, are probably due to transitions between the V_2-C_1 bands at the X point (Fig. 7). The splitting of the valence bands at the X point is 0.22 eV in this case. However, it could be that these peaks are due to transitions at the $T_3(V_1)$- $T_1(C_1)$ point as suggested for $CuGaSe_2$ crystals in [39]. An A_6 maximum was observed at 5.16 eV in [17], while an (*E1*(B)) maximum was revealed at 4.89 eV (E⊥c) in ellipsometry spectra measured at 300 K [39] which was attributed to transitions at the T point.

Since according to theoretical and experimental data [17, 18, 20] the interband interval at the N point is higher that the respective intervals at the X, P and Z points, one can consider that the peaks a_7 (5.261/5.261 eV) and e_7 (5.104/5.104 eV) observed in E||c and E⊥c polarizations, respectively, are due to transitions from the V_1 band to the C_1 band at the N point. The peaks a_8 (5.331/5.331 eV) and e_8 (5.290/5.290 eV) observed in E||c and E⊥c polarizations, respectively, are probably due also to transitions at the $N(V_2)$-$N(C_1)$ point. The maxima a_9 (5.602/5.602 eV) and e_9 (5.491/5.491 eV) are observed in the reflectivity spectra in the more short-wavelength spectral region. These features can be assigned to $N(V_3)$-$N(C_1)$ transitions.

Figure 7 presents the results of theoretical band structure calculations [25] and the interpretation of experimentally observed interband transitions in $CuAlSe_2$ crystals. The values of energies of direct interband transitions and the damping parameters for $CuAlSe_2$ crystals are summarized in Table 2.

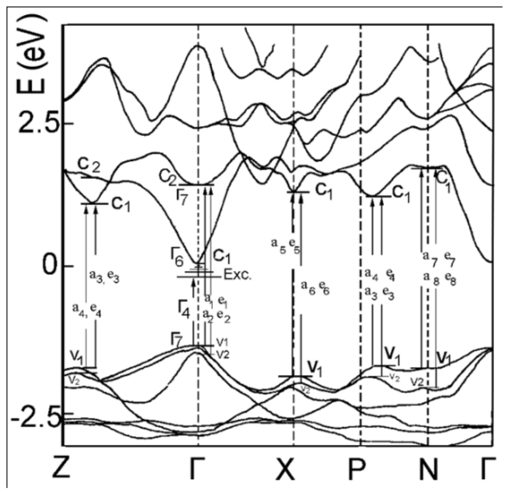

Fig. 7. Electronic transitions and the energy band structure of $CuAlSe_2$ crystals [25].

6. Conclusions

The calculations of the contours of reflectivity spectra in a wide energy interval performed in this work for $CuAlSe_2$ crystals on the basis of Kramers-Kronig relations give additional information for the interpretation of electronic transitions. However, theoretical calculations of the energy band structure at all points of the Brillouin zone are needed for a reliable interpretation of the experimentally observed electronic transitions. The ab initio calculation of the spectral dependence of the dielectric function and its comparison with the experimentally obtained spectra would be especially valuable.

References

[1] J.L. Shay and J.H. Wernick, Ternary Chalcopyrite Semiconductors: Growth, Electronic Properties, and Applications, Pergamon, Oxford, 1975.
[2] R.W. Birkmire and E. Eser, Annu. Rev. Mater. Sci. 27, 625, (1997).
[3] K. Ramanathan, M.A. Contreras, C.L. Perkins, S. Asher, F.S. Hasoon, J. Keane, D.Young, M. Romero, W. Metzger, R. Noufi, J. Ward, and A. Duda, Prog. Photovoltaics 11, 225, (2003).
[4] M.-S. Jin, C.-S. Yoon, and W.-T. Kim, J. Phys Chem. Solids 57, 1359, (1996).
[5] I.V. Bodnar, V.Yu. Rudi, and Yu.V. Rudi, Fiz. Tekh. Poluprov. 28, 1755, (1994).
[6] E.P. Zaretskaya, V.F. Gremenok, Yu. Rud, V.Yu.Rud, and S.Schorr, Book of Abstracts, 16th International Conf. on Ternary and Multinary Compounds, Sept. 15-19, 2008, Berlin.
[7] S. Chichibu, T. Mizutani, K. Murakami, T. Shioda, T. Kurafuji, H. Nakanishi, S. Niki, P.J. Fons, and A.J. Yamada, J. Appl. Phys. 83, 3678, (1998).
[8] M.I. Alonso, K. Wakita, J. Pascual, M. Garriga, and N. Yamamoto, Phys. Rev. B 63, 075203, (2001).

[9] S. Schuler, S. Siebentritt, S. Nishiwaki, N. Rega, J. Beckmann, S. Brehme, and M. Ch. Lux-Steiner, Phys. Rev. B 69, 045210, (2004).
[10] S. Siebentritt, I. Beckers, T. Riemann, J. Christen, A. Hoffmann, and M. Dworzak, Appl. Phys. Lett. 86, 091909, (2005).
[11] C.A. Durante Rincón, E. Hernández, M.I. Alonso, M. Garriga, S.M. Wasim, C. Rincón, and M. León, Materials Chemistry and Physics 70, 300, (2001).
[12] T. Kawashima, S. Adachi, H. Miyake, and K. Sugiyama, J. Appl. Phys. 84, 5202, (1998).
[13] N.N. Syrbu, I.M. Tiginyanu., L.L. Nemerenko, V.V. Ursaki, V.E. Tezlevan, and V.V. Zalamai, J. Phys. Chem. Sol. 66, 1974, (2005).
[14] N.N. Syrbu, M. Bogdanash, V.E. Tezlevan, and I.G. Stamov, J. Phys: Condens. Matter 9, 1217 (1997).
[15] N.N. Syrbu, I.M. Tiginyanu, V.V. Ursaki, V.E. Tezlevan, V.V. Zalamai, and L. L. Nemerenko, Physica B 365, 43, (2005).
[16] E. Arushanov, S. Siebentritt, T. Schedel-Niedrig, M. Ch. Lux-Steiner, J. Appl. Phys. 100 (2006) 063715; J. Phys.: Condens. Matter. 17, 2699, (2005).
[17] S. Levcenko, N.N. Syrbu, V.E. Tezlevan, E. Arushanov, J.M. Merino, and M. León, J. Phys. D: Appl.Phys. 41, 0055403, (2008).
[18] S. Levcenko, N.N. Syrbu, V.E. Tezlevan, E. Arushanov, S. Doka-Yamigno, Th. Schedel-Niedrig, and M. Ch. Lux-Steiner, J. Phys: Condes. Matter 19, 456222, (2007).
[19] J.E. Jaffe and A. Zunger, Phys. Rev. B 28, 5822, (1983).
[20] R. Ahuya, S. Auluck, O. Eriksson, J.M. Wills, and B. Johansson, Sol. Energy Mater. Sol. Cells 53, 357, (1998).
[21] G.F. Koster, J.O. Dimmock, R.G. Wheeler, and H. Statz, Properties of Thirty-Two Point Groups, Massachusetts Institute of Technology, Cambridge, 1963.
[22] N.N. Syrbu, A.V. Dorogan, V.V. Ursaki, and A. Masnik, J. Opt. 12, 075703, (2010).
[23] S. Shirakata, A. Ogawa, S. Isomura, and T.Kariya, Jpn. J. Appl.Phys. Suppl. 32-3, 94 (1993).
[24] A.M. Andriesh, N.N. Syrbu, M.S. Iovu, and V.E. Tezlevan, Phys. St. Sol. (b) 187, 83, (1995).
[25] S.I. Pekar, Zh. Eksp. Teor. Fiz. 34, 1176, (1958).
[26] V.M. Agranovich and V.L. Ginzburg, Spatial dispersion in crystal optics and the theory of excitons, Izd. Nauka, Moscow, 1965; Interscience, Wiley, New York, 1966.
[27] E.L. Ivchenko, Exitons, Ed. by E.A. Rasba, M.D. Struge, North-Holand Publ. Comp., 1982, p.141.
[28] A. Selkin, Phys.Status Solidi (b) 83, 47, (1977).
[29] S.A. Permogorov, V.V. Travnicov, and A.V. Selkin, Fiz. Tverdogo Tela 14, 3642, (1972).
[30] J.C. Rife, R.N. Dexter, P.M. Bridenbaugh, and B.W. Veal, Phys. Rev. B 16, 4491, (1997).